JOURNAL OF MATERIALS SCIENCE 27 (1992) 1369–1374

Residual stress effect on impact properties of Gr/Al metal matrix composite

JI-LIANG DOONG
Department of Mechanical Engineering, National Central University, Chung-li, Taiwan 32054
SHYH-NUNG S. LIN, H. L. MARCUS
Center for Materials Science and Engineering, The University of Texas at Austin, Austin, TX 78712, USA

The effects of residual stress on the impact properties of the unidirectionally reinforced P 100 Gr/6061 Al metal matrix composites with different thermal histories have been investigated using an instrumented impact test method and scanning electron microscopy. The cantilever impact generally causes tensile failure at the notch and compressive loading on the opposite side of the specimen. The specimens with yield tensile matrix residual stresses have planar fracture surfaces and low impact energy due to the contribution of tensile residual stress. The specimens with small residual stresses have moderate impact energy because debonding between fibre and matrix or fibre/matrix separation also serves as an additional mechanism for energy absorption. The specimens with higher compressive matrix residual stresses have the largest maximum load of all the specimens with the same matrix treatment. The specimen with matrix compressive yield residual stress has the maximum impact energy owing to a stepwise fracture surface. It can be concluded that good impact properties of composite materials can be obtained by choosing a suitable thermal history to modify the deleterious tensile matrix residual stress.

1. Introduction

Metal matrix composites (MMC) provide a relatively new way of strengthening metals and they are recognized to have the potential for high-temperature application while maintaining usable levels of fracture strength. However, a residual thermal stress can build up because of a difference in thermal expansion coefficients of the fibre and the matrix when cooling from high processing temperatures. Owing to the large thermal mismatch in the fibre longitudinal direction, the thermal stress can be large enough to cause yielding in the matrix. For example, the combination of graphite fibres with slightly negative coefficient of thermal expansion (CTE) and aluminium matrix with high positive CTE leads to a plastic flow in the matrix and large internal stresses in the constituents even for a relatively small temperature change [1]. The estimation of residual stress is required to evaluate the performance of MMC. There have been a few studies [2–5] to estimate the thermal residual stresses. Some research has focused on experimental measurements of residual stresses [6–8]. It is well recognized that the state of stress affects the performance of these composites. The effect of the thermally induced residual stresses on the yield behaviour has been discussed by Wakashima *et al.* [9]. However, there has been very little work reported on the effects of residual stresses on dynamic responses of MMC materials.

Understanding the impact response of composites has become an area of great academic and practical interest [10–14]. It is well known that the mechanical properties and the fracture mechanisms of composites with residual stresses are different from those of materials without residual stresses, because of the superimposition effect of the residual stresses with the applied stresses. In addition, fibre composites are highly susceptible to internal damage caused by impact loading. It is therefore necessary that this effect should be studied in more detail.

The impact response of composites reflects a failure process involving crack initiation and crack growth in the elastic/plastic matrix, fibre breakage and pull-out, delamination, and debonding. The instrumented impact test is potentially a more useful tool for evaluating the dynamic response of materials mainly because the traditional Charpy and Izod impact tests could not provide such information. The force–displacement curves of the test specimen during impact can be recorded by a computer-controlled data acquisition system and then analysed. The shape of the curve provides information on the initiation, yielding, and propagation energy during impact.

The purpose of the present study is to investigate the effects of thermal residual stresses on the impact properties of MMC P100Gr/6061Al using an instrumented impact tester. The test specimens with various residual stresses can be obtained via heat treatments of the aluminium matrix composite. Scanning electron microscopy is applied to study the microstructural failure mechanisms.

2. Experimental procedure

A unidirectionally reinforced double-ply pitch P 100 Gr/6061 Al MMC plate for this study has a total thickness of 0.81 mm, with 6061 Al face sheets of thickness 0.1 mm on both sides. Fibre volume fraction of the composite, V_f, is about 40%. A detailed description of residual stress estimation by X-ray diffraction was presented elsewhere [15, 16]. The specimen number, thermal histories, and residual stresses are shown in Table I.

The drop-weight impact tests were conducted on a Dynatup Model 8200 with GRC 730-I automated data acquisition and analysis system. The striking tup and the anvil of the tester were designed according to the ASTM standard for Charpy test. The specimen dimensions were 80 mm long by 10 mm wide and a 2 mm depth notch was machined at the centre of the length. The hammer and tup weighed 9.55 kgf. The impact velocity was set at 1.83 m s^{-1}. The critical parameters which were used to compare the impact response of each material include: (a) maximum load, P_m; (b) energy absorbed to maximum load (end of damage initiation phase), E_m; (c) total absorbed energy for through-penetration, E_t; and (d) the energy absorbed in the propagation phase, $E_p = E_t - E_m$ and the ductility index, DI, equal to E_p/E_m. The measurement data are summarized in Table II and typical impact response of force–time diagrams are shown in Fig. 1.

A Jeol 35 SEM using a 25 keV primary beam was used for the microstructural studies. The specific features in the micrographs of each tested specimen will be discussed in the next section.

3. Results and discussion

3.1. Residual stress effect

The previous microstructural studies [15, 16] revealed that maximum residual stresses of the composite were determined by the yield strength of the aluminium matrix which was different from the monolithic alloy. The maximum residual stresses measured at any quenching temperature are approximately 100 and 140 MPa for Al-T4 and Al-T6 treatments, respectively. The residual stresses measured in the aluminium alloy matrix were found to be in good agreement with the calculated results of Rice *et al.* [17] using finite element methods. The stress of the fibre is opposite to that of the matrix [18, 19]. For the case of uniaxial, uniform displacement, thermal stress changes in both phases. The approximate relationship between the matrix stress change, $\Delta\sigma_m$, and fibre stress change, $\Delta\sigma_f$, can be expressed as

$$\Delta\sigma_f V_f = -\Delta\sigma_m(1 - V_f) \quad (1)$$

For these composites with $V_f = 0.4$, the residual stress of the fibres is opposite to that measured in the matrix with a magnitude of 1.5 times as large. It means that interfacial shear stress between fibre and matrix increases with the matrix residual stresses. For example, the residual stresses of specimen with T6-1 treatment are 140 and -210 MPa for matrix and fibre, respectively. The stress difference is 350 MPa. For a specimen with T6-3 treatment, the stress difference is only 15 MPa. In addition, interface debonding will occur if the interfacial bonding is not strong enough to withstand the shear stress resulting in the pull-out phenomenon. All these cause the failure of the composite materials. Therefore, the residual stress of composites should be reduced to as low as possible. Owing to the superimposed effect of residual stresses on the applied load, the compressive residual stress has a retarding effect on fatigue crack growth [20, 21].

The cantilever impact on the specimens causes tensile failure at the notch and compressive loading at the surface opposite to the notch. The crack initiation and propagation occurs at the notch. Thus when compressive residual stresses are present in the matrix, the applied stress must overcome them first so that the fracture can take place. In contrast, tensile residual stresses in the matrix accelerate the fracture.

3.2. Impact response

Golovoy *et al.* [22] investigated the impact response of laminate composites and indicated that tensile failure is the major mechanism in the initiation stage. Fracture propagation involves both tensile and shear

TABLE I Residual stresses of graphite fibres in P100/6061 Al matrix with various thermal histories

Specimen number	Solution treatment (°C) (h)	Ageing treatment (°C) (h)	Quenching[a] temperature (°C)	Residual stress (MPa)
T4-1	530 2	None	20.0(RT)	93
T4-2	530 2	None	− 78.5	3
T4-3	530 2	None	− 117.0	− 46
T4-4	530 2	None	− 196.0	− 78
T6-1	530 2	160 18	20.0(RT)	140
T6-2	530 2	160 18	− 78.5	30
T6-3	530 2	160 18	− 117.0	− 6
T6-4	530 2	160 18	− 196.0	− 30

[a] Four different thermal histories were used with various quenching temperatures after ageing treatment and then back to room temperature (20 °C).

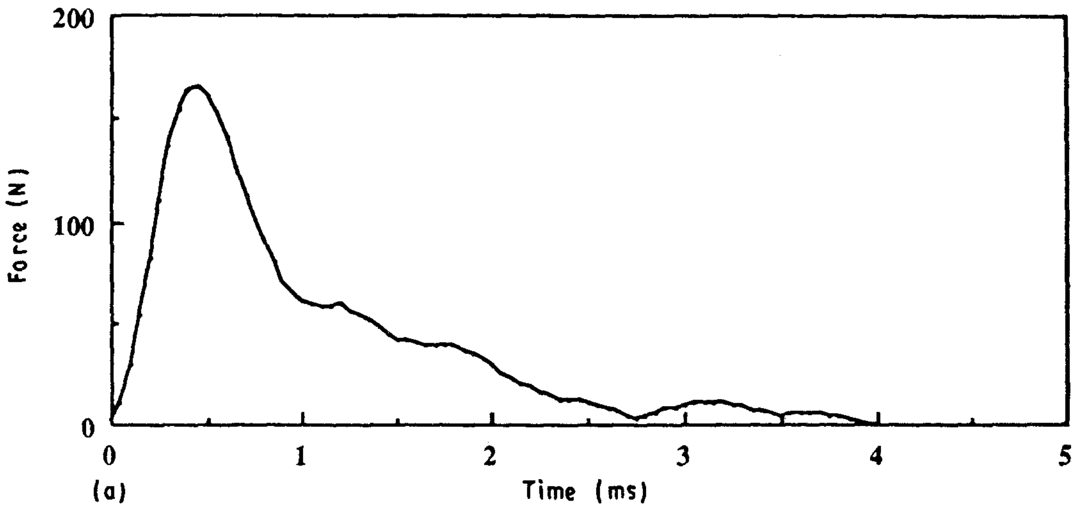

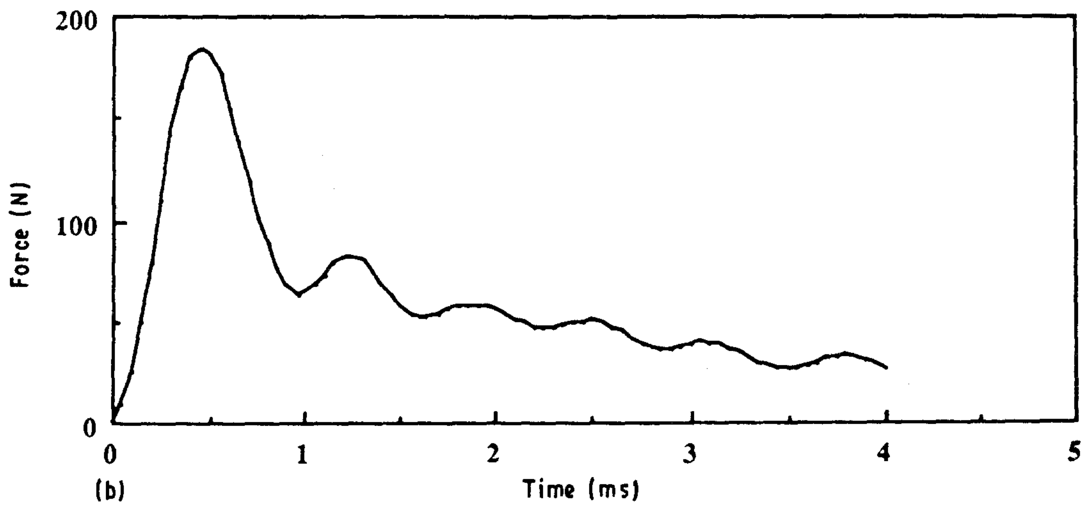

Figure 1 The force–time-impact response diagrams of specimens (a) T4-1, (b) T4-4.

TABLE II The effect of residual stress on the composite impact properties

Specimen number	Maximum load (N)	t_m (ms)	E_m (J)	E_p (J)	E_t (J)	DI
T4-1	180.58	0.350	0.0758	0.2144	0.2902	2.8298
T4-2	195.60	0.350	0.0691	0.5798	0.6489	8.3957
T4-3	199.34	0.350	0.0817	0.3697	0.4514	4.5238
T4-4	199.52	0.400	0.1045	0.5500	0.6545	5.2610
T6-1	189.63	0.350	0.0733	0.2567	0.3300	3.5001
T6-2	192.61	0.325	0.0764	0.4839	0.5603	6.3308
T6-3	193.10	0.450	0.0973	0.4599	0.5572	4.7266
T6-4	217.47	0.350	0.0853	0.2981	0.3834	3.4947

failure, which is simply by successive delamination along planes parallel to the midplane. This statement can be used to explain partially the impact response of some specimens with large propagation energy, E_p. From Table II, the residual stress free specimens T4-2 and T6-3 show significantly higher absorption energy than the specimens T4-1 and T6-1 with yield tensile residual stresses in the matrix. The lower impact energy mode is caused by the larger tensile matrix residual stresses. This can be demonstrated by observing the side fracture surface of the specimens (see Fig. 2). The differences in the macrographs of the fracture surfaces in Fig. 2 clearly show the influence of residual stress on the impact response of the present composite materials. With large matrix tensile stress, the fracture is planar but with near free or large compressive matrix stresses, more shear fracture is observed.

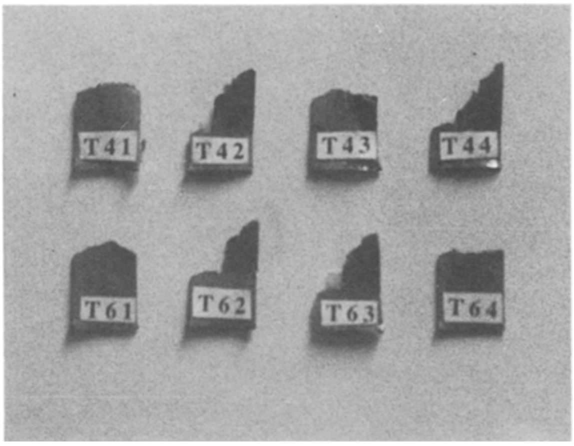

Figure 2 Side fracture surfaces with T4 and T6 treatments.

It has been argued by Jang *et al.* [23], that the matrix should be the dominant factor with only a small amount of fibre breakage prior to maximum loading. Near the maximum loading and soon after that, fibre breakage dominates. This suggests that extensive fibre breakage occurs at the end of the initiation phase of the impact loading. The considerable tensile residual stress in the matrix can promote the initiation stage of fracture at the crack tip to reduce the maximum impact loading of composite materials. Fig. 3 indicates the effect of matrix residual stress on carrying load. As the strain increases, the crack tip, the tensile yielded matrix no longer will carry additional load, resulting in excess stress in the fibre. This leads to fibre breakage in a colinear manner with the crack resulting in the planar fracture surface shown in Fig. 4. When the matrix has a compressive yield residual stress, it can carry a significant fraction of the load at the crack tip and the fibres which are in a tensile residual stress condition will fracture noncolinearly with cracking. The net result is a great deal of shear deformation and fibre pull-out along the continuous fracture path (Fig. 5). For intermediate residual stress level, a mixture of the two failure mechanisms was observed. All the above would be equally true for T4 and T6 treatments.

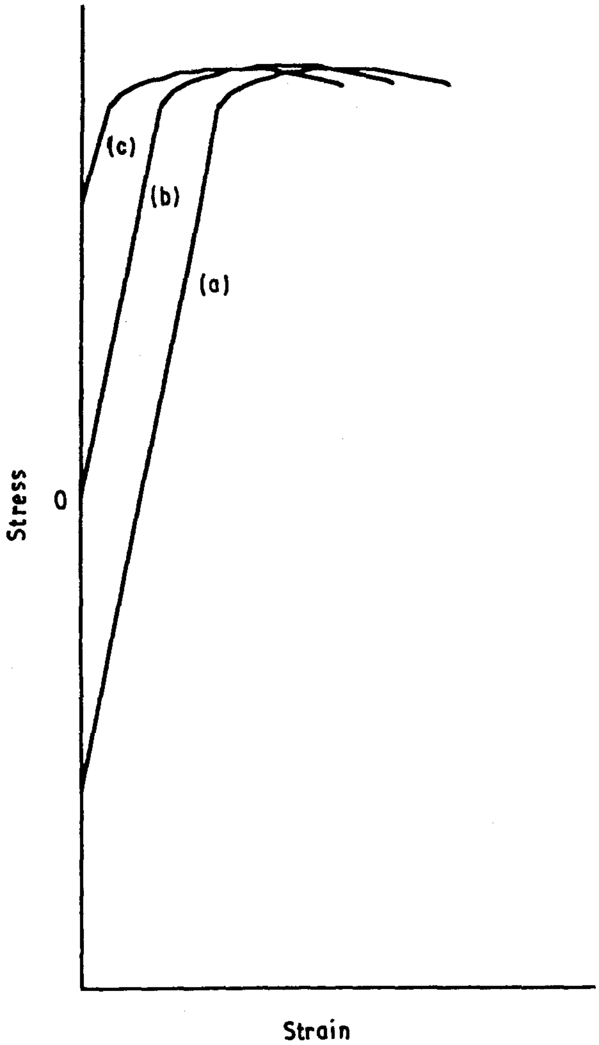

Figure 3 Matrix residual stress effect on the matrix stress–strain curve (a) compressive residual stress; (b) free residual stress; (c) tensile residual stress.

3.3. Microstructural failure analysis

In general, the possible operating microfailure mechanisms during impact loading include matrix cracking, fibre–matrix debonding, fibre breakage, and fibre pull-out. The work of fracture includes (i) a small contribution from the fracture energy of fibre and matrix, (ii) the debonding energy and (iii) the pull-out energy. From the studies by Kelly [24] and Outwater etc. [25], it is shown that the work done on separating fibres and matrix can make a major contribution to the total energy of fracture. The mechanism of pull-out is a more significant one than the debonding mechanism as an energy absorber. However, debonding must occur before pull-out, but can be a result of noncolinear fibre breakage. These observations are in agreement with the impact test of the matrix tensile residual stress specimens which have the lowest maximum loading and initiation energy. The micrographs of T6-1 and T4-1 specimens have similar fracture pattern as shown in Fig. 4, on the microstructural level. The fracture surface is planar. Owing to the matrix yield tensile residual stress effect as discussed previously, the fibres break before extensive separation of the fibres from the matrix leading to a smaller amount of pull-out and thus less absorbed energy [24, 25].

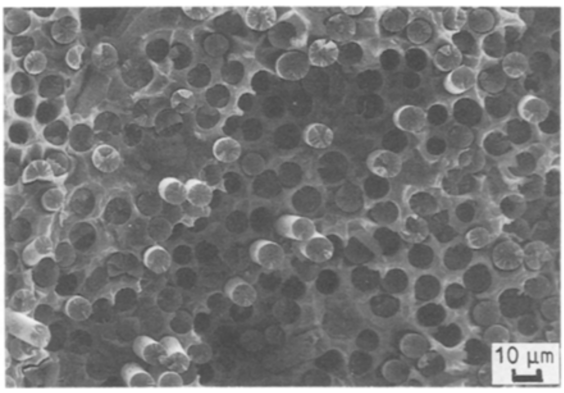

Figure 4 Fracture surface of specimen T6-1.

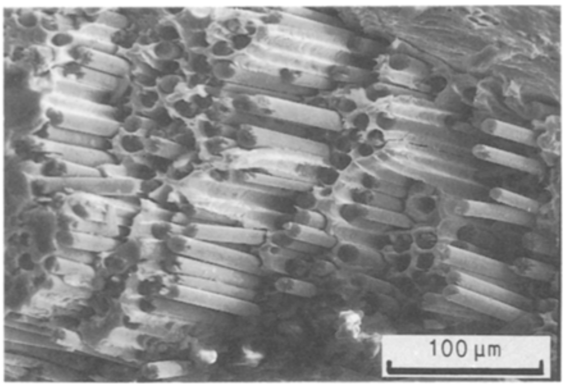

Figure 5 Fracture surface of specimen T4-4.

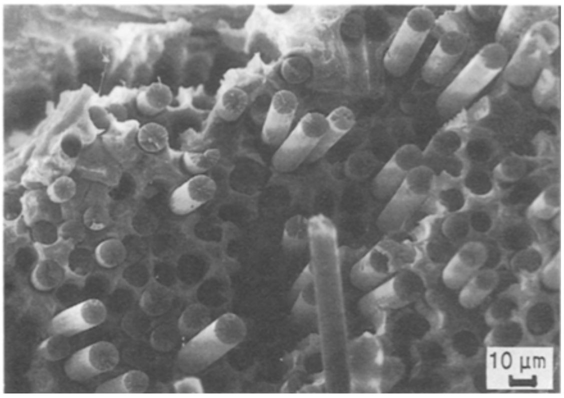

Figure 6 Fracture surface of specimen T6-4.

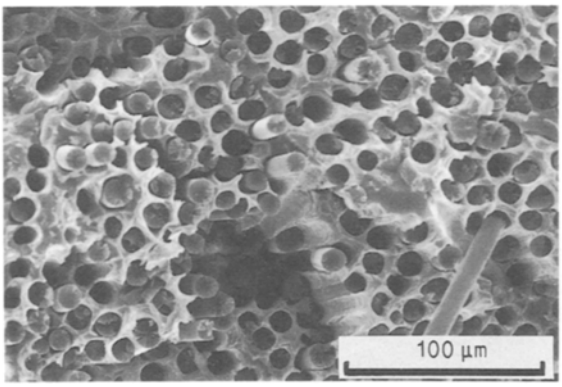

Figure 7 Fracture surface of specimen T4-2.

On the contrary, the specimen T4-4 with large compressive matrix residual stress has a stepwise fracture surface shown in Fig. 5. As described earlier, the matrix can carry some of the applied load. Meanwhile the fibre tensile stress will increase until the matrix reaches the yield stress state. Just as shown in Fig. 3, the fracture strain of T4-4 is larger than that with yield tensile residual stress in the matrix. From the viewpoint of statistics, the possibility of fibre breakage at various positions will increase and produce noncolinear fibre breakage in the fracture surface. This results in a great deal of shear deformation and fibre pull-out. The force–time impact response diagram of specimen T4-4, shown in Fig. 1b, also indicates the stepwise fracture mechanism.

The micrographs of specimens T4-3, T6-2 and T6-4 with intermediate residual stresses show a mixture of the two failure mechanisms, a planar fracture surface and a stepwise fracture surface. There are some long pull-out fibres on less planar fracture surfaces which can be observed in Fig. 6. This indicates that debonding and pull-out mechanisms play some roles in the fracture processes and probably result in an increase of impact energy. For the nearly free residual stress specimens T6-3 and T4-2 (Fig. 7), dimple-like fracture surfaces with relatively short fibres extruding are observed. The appearance seems to lie between the two extremes of planar and shear deformed fracture surfaces.

4. Conclusions
Several important conclusions can be drawn. First, the specimen with yield tensile matrix residual stress has a planar fracture surface and low impact energy due to the yield tensile residual stress. Secondly, the specimens with higher compressive matrix residual stress have largest maximum load of all the same matrix treatment specimens. The specimen T4-4 with matrix compressive yield residual stress has the maximum impact energy owing to a stepwise fracture mechanism. Thirdly, specimens with relatively small residual stress have moderate impact energy because of a mixture of failure mechanisms of planar and stepwise fracture surfaces. Finally, it can be concluded that good impact properties of composite materials can be obtained by selecting an appropriate thermal treatment so that the deleterious tensile residual thermal stress can be reduced or even eliminated.

Acknowledgements
The authors thank Professor D. R. Paul, Chemical Engineering, UT-Austin, for permission to use the instrumented impact tester, and T. W. Cheng, Chemical Engineering, UT-Austin, for help with instrument setup and data acquisition. Research partially supported by ONR Grant N00014-90-5-1164.

References
1. S. D. TSAI, D. MAHULIKAR, H. L. MARCUS, I. C. NOYAN and J. B. COHEN, *Mater. Sci. Engng* **47** (2) (1981) 145.
2. S. S. HECKER, C. H. HAMILTON and L. J. EBERT, *J. Mater. JMLSA* **5** (1970) 868.
3. M. VEDULA, R. N. PANGBORN and R. A. QUEENEY, *Composites* **19** (1988) 55.
4. *Idem.*, *ibid.* **19** (1988) 133.
5. Y. H. PARK and H. L. MARCUS, in "Mechanical behavior of metal matrix composites", edited by J. E. Hack and M. F. Amateau, Conference Proceedings of the Metallurgical Society of AIME and the Material Science Division of ASM (American Institute of Mining, Metallurgical, and Petroleum Engineerings, New York, 1983) pp. 77–81.
6. C. N. J. WAGNER, M. S. BOLDRICK and V. PEREZ-MENDEZ, *Adv. X-Ray Anal.* **26** (1982) 275.
7. E. MACHERAUCH and U. WOLFSTIEG, *ibid.* **20** (1977) 369.
8. V. M. HAUK, R. W. M. OUDELHOVENS and G. J. H. VAESSEN, *Metall. Trans.* **13A** (1982) 1239.
9. K. WAKASHIMA, T. KAWAKUBO and S. UMEKAWA, *ibid.* **6A** (1975) 1755.

10. J. D. WINKEL and D. F. ADAMS, *Composites* **16** (1985) 268.
11. C. K. L. DAVIES, S. TURNER and K. H. WILLIAMSON, *ibid.* **16** (1985) 279.
12. S. L. KESSLER, G. C. ADAMS, S. B. DRISCOLL and D. R. IRELAND (eds), Instrumented Impact Testing of Plastics and Composite Materials, ASTM STP 936 (American Society for Testing and Materials, Philadelphia, 1987).
13. J. S. WU, K. FRIEDRICH and M. GROSSO, *Composites* **20** (1989) 223.
14. M. N. GHASEMINEJHAD and A. PARVIZI-MAJIDI, *ibid.* **21** (1990) 155.
15. H. S. PARK, Doctorial dissertation, University of Texas Austin, TX (1989).
16. H. S. PARK, J. L. DOONG and H. L. MARCUS, submitted to *J. Mater. Sci. Engng.*
17. M. H. RICE, A. MAEWAL and G. A. GURTMAN, "The effects of residual stresses on the X-Ray induced response of metal matrix composites", DNA report (SSS-FTR-89-10219) 1989.
18. H. M. LEDBETTER and M. W. AUSTIN, in "Residual Stress in Science and Technology", edited by E. Macherauch and V. Hauk, International Conference on Residual Stresses, 1986 (Garmisch-Partenkirchen, FRG, 1987, DGM Informationsgesellschaft, Germany) pp. 517–21.
19. Y. IKEUCHI and H. FUJIWARA, *ibid.*, pp. 523–30.
20. H. GRAY, L. WAGNER and G. LUTJERING, *ibid.*, pp. 815–22.
21. J. L. DOONG, T. J. CHEN and Y. H. TAN, *Engng Fract. Mech.* **33** (1989) 483.
22. A. GOLOVOY, M. F. CHEUNG and H. van OENE, "The impact behavior of glass and carbon fiber composites", Ford Research Technical Report SR-83-138 (Ford Motor Co., Dearborn, MI, 1983).
23. B. Z. JANG, L. C. CHEN, L. R. HWANG, J. E. HAWKES and R. H. ZEE, *Polym. Compos.* **11** (1990) 144.
24. A. KELLY, *Proc. R. Soc. Lond.* **A319** (1970) 95.
25. J. O. OUTWATER and M. C. MURPHY, "Fracture energy of unidirectional laminates", Proceeding of the 24th SPI/RP Conference, paper 11-B (Society of the Plastics Industry, New York, 1969).

Received 7 January and accepted 13 May 1991